DEUTSCHES ELEKTRONEN-SYNCHROTRON DESY

DESY 85-055
June 1985

GENERAL FEATURES OF JETS IN e^+e^--ANNIHILATION

by

P. Mättig

Deutsches Elektronen-Synchrotron DESY, Hamburg

ISSN 0418-9833

NOTKESTRASSE 85 · 2 HAMBURG 52

To be sure that your preprints are promptly included in the
HIGH ENERGY PHYSICS INDEX ,
send them to the following address (if possible by air mail) :

DESY
Bibliothek
Notkestrasse 85
2 Hamburg 52
Germany

DESY 85-055
June 1985

ISSN 0418-9833

GENERAL FEATURES OF JETS IN e^+e^- - ANNIHILATION[1]

P. MÄTTIG

DESY , Hamburg, FRG

It is hoped that general features of jets will enlighten a region in space-time which up to now is not well understood. Hadron production in e^+e^--annihilation offers a simple and clear way to examine how quarks turn into hadrons. Space-time development of the process can be divided into four separate regions as is sketched in fig. 1. The measurement of the quark form factor shows that quarks are pointlike down to distances of at least $7 \cdot 10^{-17} cm$ [1]. Resolving possible structures beyond this region will be one of the prime goals of the next generation of accelerators, especially the ep-collider HERA being built at DESY. Between $0.001 fm$ and $\sim 0.05 fm$ (corresponding to masses of $\sim 4\ GeV$, the typical mass of an experimentally resolvable jet) the quarks can emit a hard gluon which is the origin of a separate jet. In this region perturbative QCD works remarkably well. At a distance of $\sim 1\ fm$ from the interaction point hadrons exist and are bundled into jets that can be seen in the detectors. Between these two regions fragmentation

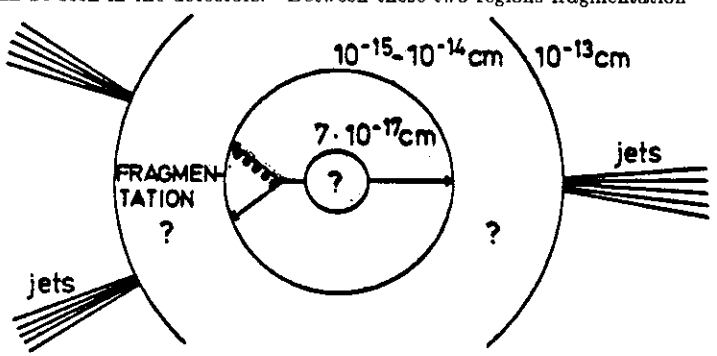

Fig.1

occurs and much work has been devoted to the questions of how the quarks convert into hadrons and what happens between 0.05 and 1 fm. No detailed theoretical prediction exists for this region, only models and phenomenological ideas based on soft QCD- effects or statistical assumptions. One of the prime goals in measuring

[1]Invited talk at the First International Workshop on Local Equilibrium in Strong Interaction Physics (LESIP I) in Bad Honnef, Federal Republic of Germany, September 3-6, 1984

the general structure of jets in e^+e^--annihilations is to obtain information on this region.

Many facts have been gathered during the last years at PETRA and recently also at PEP. Jets occur in other types of reactions as $pp/p\bar{p}$-collisions or deep inelastic lepton-nucleon scattering as well. However e^+e^--annihilation has the special advantage that (a) no hadronic matter exists in the initial state that can influence quark fragmentation, and (b) the kinds of partons in the first stage of fragmentation are unique - all jets originate from quarks, no gluons or diquarks are around at the very first stage. One important result is that the c.m. energy W effective in the partonic reaction is uniquely known.

Data on fragmentation in e^+e^- - annihilations have by now been accumulated at several energies W with rather high statistics allowing not only a thorough analysis of jet properties at fixed W but also of their variation with W. Most of the data presented in the following sections are corrected for detector effects and experimental cuts.

Multiplicity distributions.

We start with the discussion of results on multiplicity distributions per event and per jet [2].

The dependence of the average number of charged particles $< n_{CH} >$ on the total c.m. energy W for both e^+e^-- and $pp/p\bar{p}$-collisions can be seen in fig. 2. The e^+e^- - multiplicities are systematically higher than those obtained in $pp/p\bar{p}$- collisions at the same W. This is a well known feature and methods have been developed to define some 'effective' W for pp-collisions, leading to a closer agreement between the distributions of these two reactions. Both distributions show a rise with W which is much stronger than a pure logarithmic dependence

$$< n_{CH} >= a + b \cdot \ln s$$

(with $s = W^2$) as was anticipated for Feynman scaling. More appropriate parametrisations are

a. $< n_{CH} >= a + b \cdot \ln s + c \cdot (\ln s)^2$ which was found empirically to be well suited to describe the $< n_{CH} >$ dependence in pp-collisions [3]. For e^+e^- - data a fit leads to

$$a = 3.33 \pm 0.11\ ,\ b = -0.40 \pm 0.08\ ,\ c = 0.26 \pm 0.01$$

and its result is shown by the full curve in fig.2.

b. $< n_{CH} >= a \cdot s^{1/4}$ Such a distribution was suggested from phase space considerations [4]. The fit gives

$$a = 2.18 \pm 0.01$$

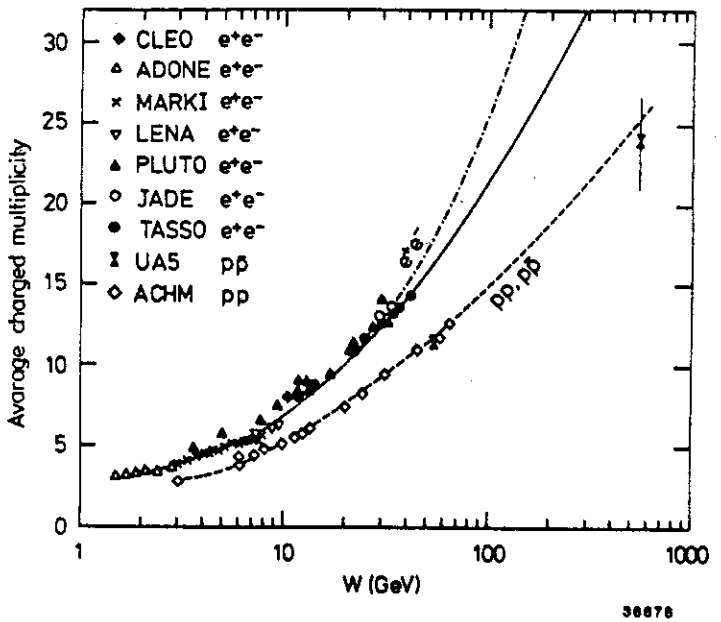

Fig. 2

and leads to a prediction very similar to the $(\ln s)^2$-parametrisation.

c. From QCD-shower calculations a rise in the particle multiplicity of the form

$$< n_{ch} >= a + b \cdot exp(c \cdot \sqrt{\ln s})$$

is suggested [5]. The fit result is reproduced by the dashed-dotted curve in fig. 2 with

$$a = 2.71 \pm 0.08\ ,\ b = 0.058 \pm 0.010\ ,\ c = 1.97 \pm 0.06.$$

This parametrisation predicts the largest multiplicities at the higher energies.

All these parametrisations describe the data quite well[1] . None of these can

[1]For these fits a systematic error of 5% for each individual measurement was assumed, however no correlations of these errors within the same experiment were taken into account because they are not obtainable from the relevant publications.

be ruled out at the moment and it seems that even at LEP-energies it will be very difficult to discriminate between these alternatives.

In fig. 3 the charged multiplicity distribution at W=14, 22 and 34 GeV

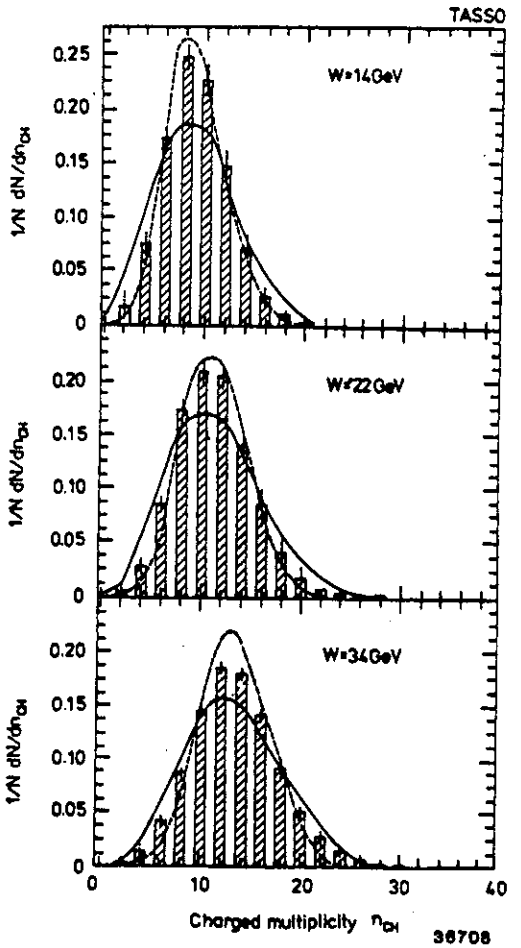

Fig. 3

is shown. For an uncorrelated production mechanism one expects a Poisson-

distribution

$$p(i) = 2 \cdot \frac{\lambda^i}{i!} \cdot e^{-\lambda}$$

where p(i) is the probability for an event to have the multiplicity i and λ is the average charged multiplicity. These distributions are represented by the dashed line in fig. 3. The curves are narrower than the data. Due to charge conservation the number of negative particles has to be the same as the number of positive particles suggesting instead of the formula above

$$p(i) = \frac{(\lambda/2)^{i/2}}{(i/2)!} \cdot e^{-\lambda/2}.$$

The resulting distribution (full line) is wider than observed. This can be taken as an indication that further constraints (e.g. energy-momentum conservation) still affect the shape of the multiplicity distribution.

From Feynman-scaling Koba, Nielsen and Oleson [6] derived that for $s \to \infty$, $< n > p(n)$ should be a function of $\frac{n}{<n>}$ only, independent of W. This property is known as KNO-scaling. Remarkable agreement with these predictions has been found in pp-collisions for $\sqrt{s}$ *up to* $\sim$ 60 GeV. Fig. 4 shows a compilation of the KNO-distributions measured in e^+e^--annihilations for c.m. energies W between 5 and 34 GeV[1] . The data at these different energies agree well with each other so that KNO-scaling is fulfilled to within $\sim$ 20 %.

The scaling behaviour can be more easily examined by using moments of the multiplicity distribution. In fig. 5 $\frac{<n_{CH}>}{D}$, $D = \sqrt{< n_{CH}^2 > - < n_{CH} >^2}$ is displayed for different W both for e^+e^- and $pp, p\bar{p}$-reactions. $\frac{<n_{CH}>}{D}$ for e^+e^-

[1]Similar results have also been found by the JADE-collaboration [7] and the HRS-collaboration [8].

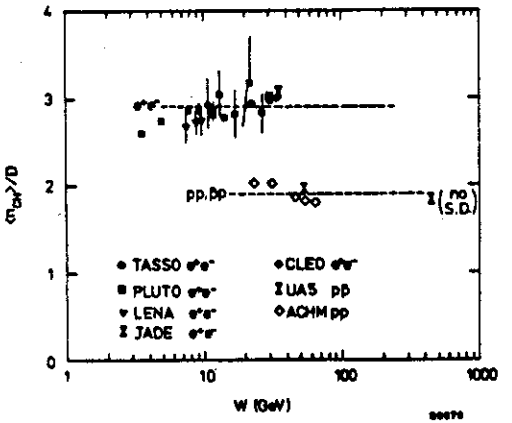

Fig.5

is about $\sqrt{2}$ higher than for $pp/p\bar{p}$ showing that not only the average value, but also the shape of the multiplicity distribution is different in both reactions. The data from e^+e^--annihilation seem to rise with W and may indicate a violation of KNO-scaling of $\sim$ 10 % between W=5 and 34 GeV. However since the statistical and systematic errors are of the order 7 – 10% , this rise is not significant.

Up to now the multiplicty distribution of the whole event was considered. Fig. 6 reproduces the multiplicity per jet for different energies. For this analysis 'jet' was set equal to all particles within a hemisphere with respect to the jet axis, no attempt was made e.g. to separate quark jets from gluon jets. Again the KNO-scaling is fullfilled to a high degree. In comparison with the KNO-distribution for the whole event the distribution for a single jet has a smaller maximum value and is narrower.

The width can be taken as an indication of how far the multiplicities in a jet are uncorrelated. Assume a Gaussian behaviour for the multiplicities

$$f(n_{CH}) = \frac{1}{\sqrt{2\pi}D} exp\left(-\frac{(< n_{CH} > - n_{CH})^2}{2D^2}\right)$$

If the multiplication of the two jets are uncorrelated

$$D_{ev} = \sqrt{2} D_{jet}$$

and trivially

$$< n_{CH} >_{ev} = 2 < n_{CH} >_{jet}$$

Thus

$$\left(\frac{< n_{CH} >}{D}\right)_{ev} = \sqrt{2}\left(\frac{< n_{CH} >}{D}\right)_{jet}$$

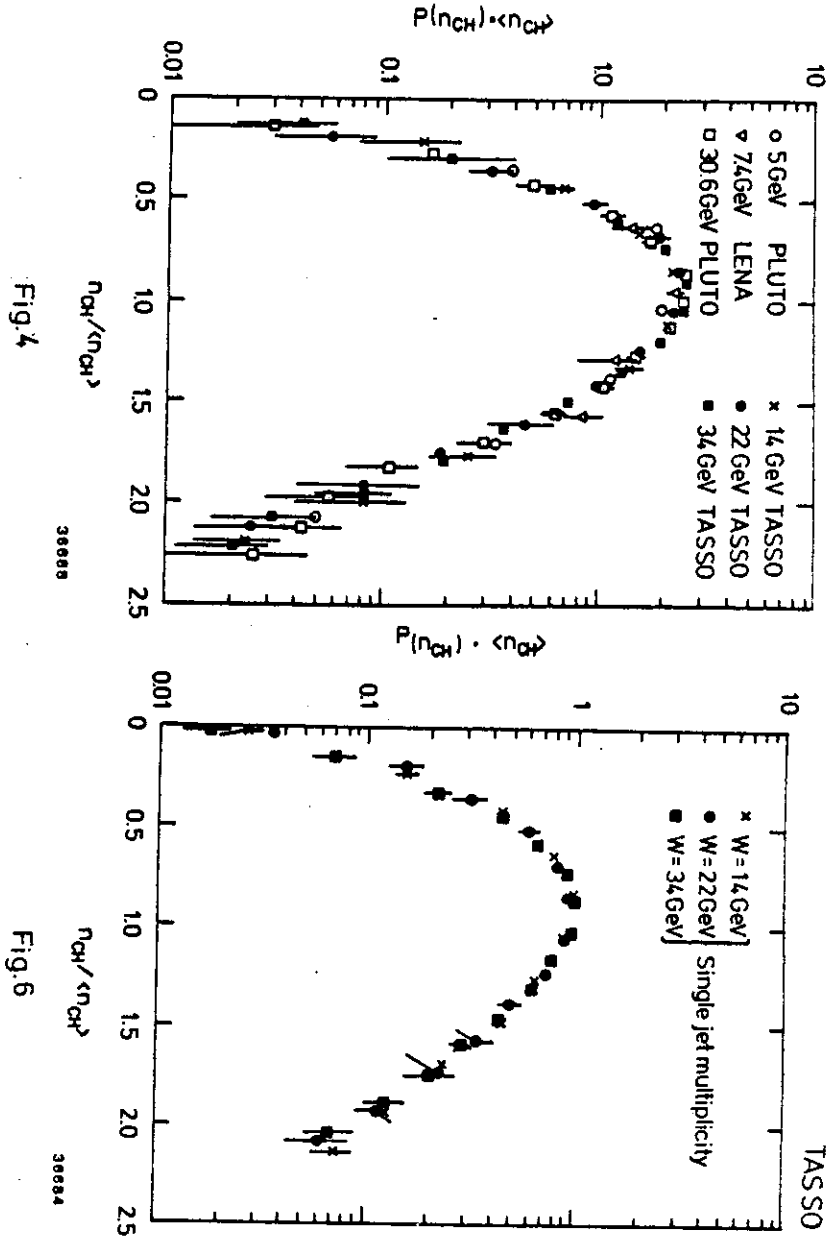

which is in rough agreement with the data yielding $\left(\frac{<n_{CH}>}{D}\right)_{ev} = 3$ and $\left(\frac{<n_{CH}>}{D}\right)_{jet} = 2.3$.

This result is in contrast to $pp/p\bar{p}$-collisions, where correlations between the multiplicities in the two jet hemispheres have been found. It is interesting to study the corresponding results for e^+e^--annihilation in more detail.

A more direct check of multiplicity correlations has been presented by W. Koch of the TASSO-collaboration some time ago [9]; a recent analysis from the HRS [8] and the TPC collaboration [10] has since confirmed his conclusions. Here we will discuss the TASSO-results. Fig. 7a shows the average uncorrected charged multiplicity in one jet (arbitrarily chosen per event) $< n_F >$ as a function of the charged multiplicity n_B of the other jet. For uncorrelated jet multiplicities $< n_F >$ should be independent of n_B. For the raw data this is obviously not the case. To study the reasons for the correlations in the data it is necessary to compare the measurement with the outcome of a model-calculation which includes fragmentation [11], decays and detector-effects. The result of this calculation is shown by the full line - it agrees well with the measurement. As in the model the quarks fragment independently from each other, this can be taken as evidence that only trivial effects lead to the correlations in the data and we can use the Monte-Carlo to examine what they are. For this analysis step by step certain features of the Model have been switched off and the resulting changes can be seen in fig.7b.

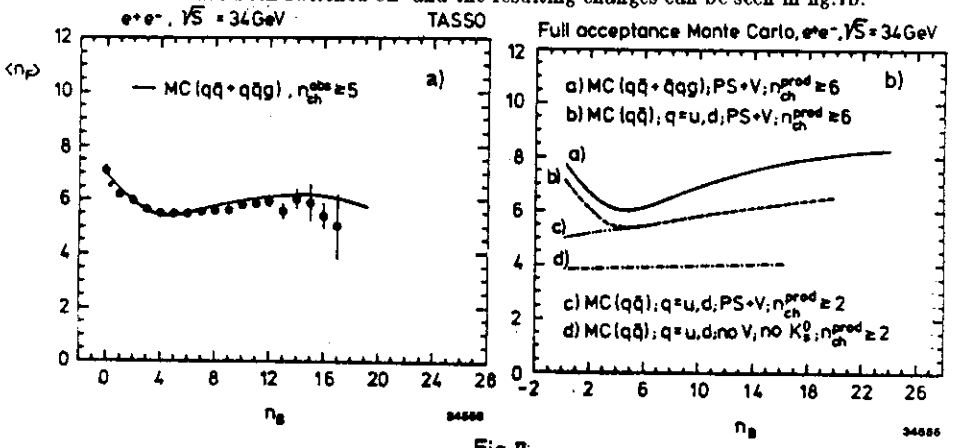

The full curve (a) reproduces the full Monte-Carlo calculation shown in fig. 7a.

- The jets from e^+e^--annihilation stem from different quark flavours and include a fraction of events with hard gluon emission. Events with different flavours and with gluon bremsstrahlung have different average multi-

plicities each [12]. To get rid of this mixture of several average multiplicities, the Monte-Carlo-calculation was restricted to produce only u and d quarks as primary partons, hard QCD corrections were omitted (curve b). The average multiplicity $< n_F >$ is reduced with respect to curve a and the curve becomes flatter for $n_B > 6$. Both effects indicate that gluon bremsstrahlung and the mixture of several flavours contribute to multiplicity correlations.

- For experimental reasons only events with more than five particles were considered in the data. Omitting this restriction in the Monte-Carlo calculation reduces the correlation for small n_B-values (curve c). Still there is a considerable $n_B - n_F$-correlation.
- This residual correlation vanishes if in addition only stable particles are generated in the Monte-Carlo (curve d). Doing this, n_F is seen to be independent of n_B. Decays can induce a correlation in the two hemispheres if e.g. a ρ^0 decays into a π^+ belonging to one hemisphere and a π^- belonging to the other.

This exercise shows that multiplicity correlations do not originate from the fragmentation process itself. Turning the argument around it indicates that fragmentation in one hemisphere is independent from the fragmentation in the other hemisphere, e.g. one of the two primary quarks fragment without 'knowing' what the other one does (as realised in the Independent Jet Model) or the string between quarks breaks up randomly in one or the other hemisphere (as in the String-model [13]).

The momentum spectrum inside jets.

More about the dynamics of jet evolution can be learnt from the examination of the momentum distribution inside jets.

The long plateau in the rapidity $y = \frac{1}{2}\ln(\frac{E+p_{||}}{E-p_{||}})$ has been known for some time to be one of the most striking features of jets. Here E is the energy of the particle, $p_{||}$ its parallel component with respect to the jet axis,[1] The rapidity distribution for different c.m. energies W is shown in fig. 8a. The distributions are nearly constant up to about $y = y_{max} - 3$, $y_{max} = \ln\frac{W}{m_\pi}$ and then drop in a similar way for the different energies. Two comments on the plateau can be made.

a. At higher energies (W=34 GeV) the particle yield at $y \approx 0$ drops by

[1]For the data to be discussed the jet axis is the thrust axis :

$$T = \max_{\vec{t}}\left(\frac{\sum \vec{p}_{||}\,\vec{t}}{\sum p}\right)$$

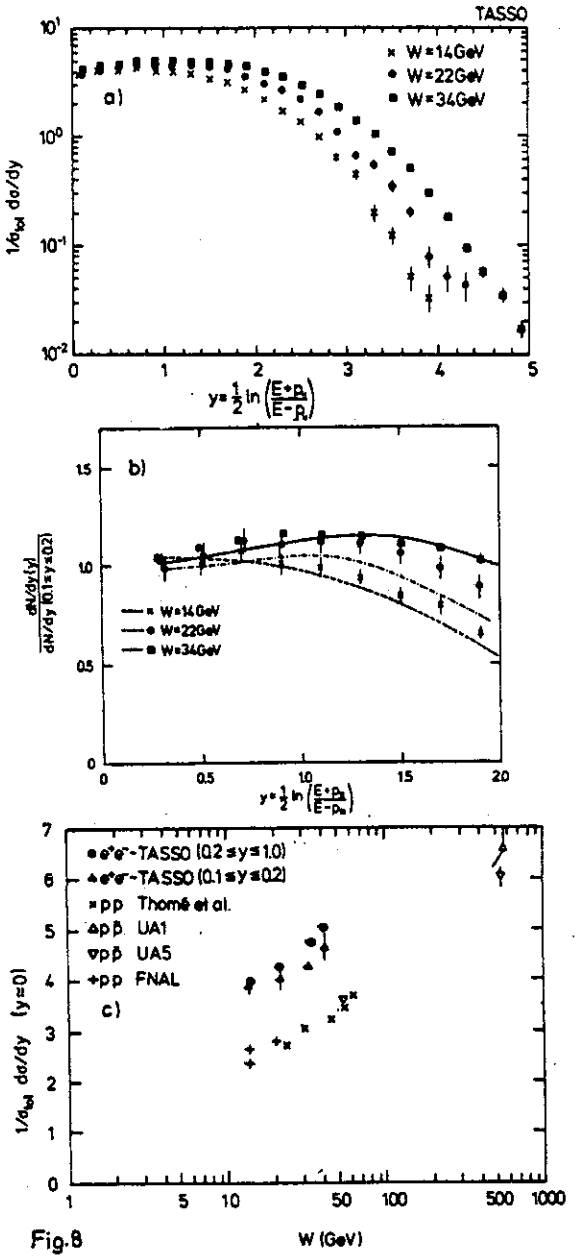

Fig.8

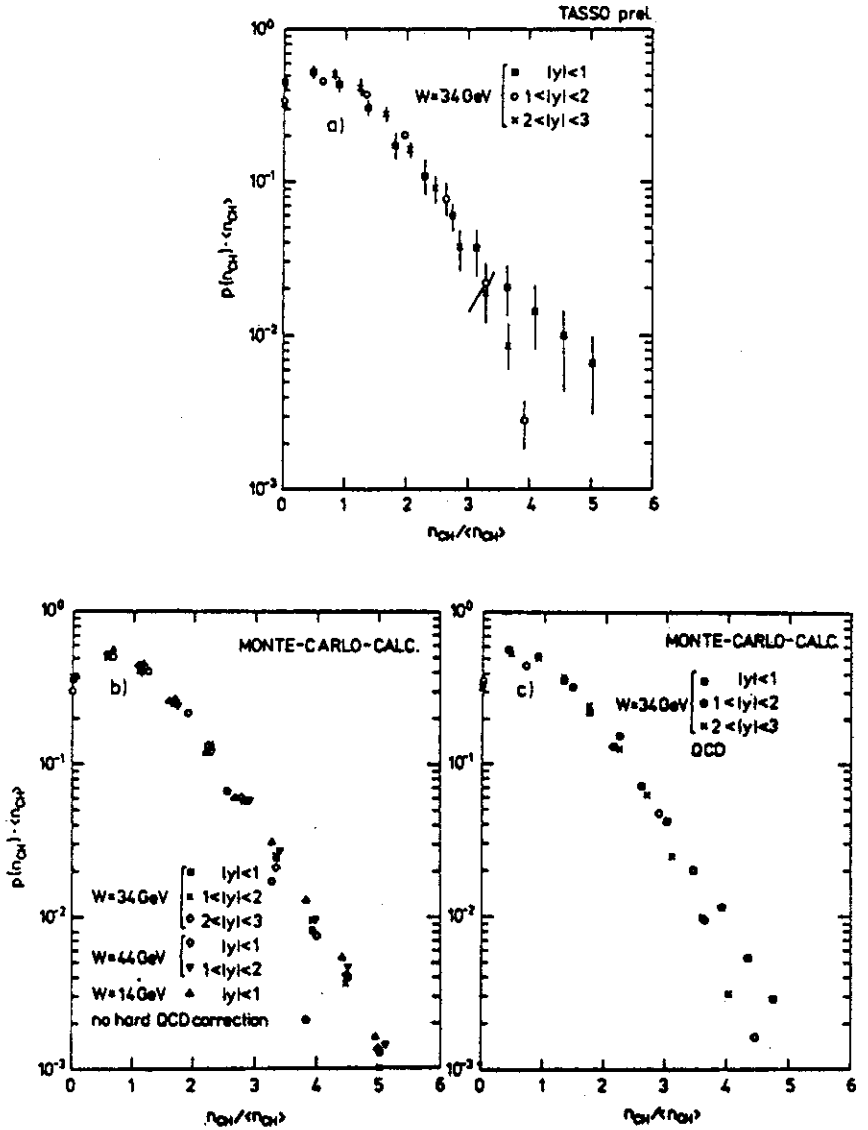

Fig.9

10 – 20% with respect to the maximum particle yield. This is more clearly seen in fig. 8b where the ratio of the particle yield at $y = y_0$ to the particle yield for $0.1 < y < 0.2$[2] is plotted for three c.m. energies. At least for W=34 GeV a steady increase in the ratio is seen with a maximum at about 1.2. In contrast the low energy data at W=14 GeV are rather flat. The general trend is reproduced by the QCD-LUND-model [13][3] and predicted by QCD-shower calculations which take into account interference terms [14].

b. The height of the plateau (i.e. the yield for $0 < y < 1$) rises with energy. This is more clearly seen in fig 8c where the height of the plateau is shown for different c.m. energies and for e^+e^--annihilation as well as $pp/p\bar{p}$-collision[1] . The rise can be parametrized by $a + b \ln W$ where b is about the same for e^+e^- and pp, a is however ~ 1.5 units higher in e^+e^-.

In the plateau region KNO-scaling is expected to hold in case of Feynman-scaling. For $p\bar{p}$-collisions violations from scaling have been seen by the UA5-collaboration [15]. Fig. 9a shows preliminary results from the TASSO-collaboration using e^+e^--annihilation data for intervals $|y| < 1, 1 < |y| < 2$ and $2 < |y| < 3$ at W=34 GeV. Note that the plateau extends up to about $|y| \sim 3$. Consistent results are found for the two intervals between $|y| = 1$ *and* $|y| = 3$, however the distribution for $|y| < 1$ shows a long tail towards high $\frac{n_{CH}}{\langle n_{CH}\rangle}$ indicating appreciable violations of KNO-scaling. As was discussed before, this is a region where QCD-effects are important and again the model calculations lead us to some understanding of the origin of this violation. Assuming fragmentation without hard QCD-bremsstrahlung leads to a particle yield in the plateau region independent of W and to a KNO-scaling for different rapidity intervals Δy for the same and for different c.m. energies (see fig. 9b). Including hard QCD-bremsstrahlung breaks this scaling behaviour, the trend of the data is reproduced : at $W = 34\ GeV$ the lowest rapidity interval shows the broadest distribution, whereas the multipliicty distributions for the intervals between $y = 1$ and $y = 3$ are in good agreement with each other. Thus the long tail in the multiplicity distribution seems to be a result of hard gluon bremsstrahlung.

One of the most striking features of hadron production in e^+e^- -annihilation at $W \sim 30 GeV$ is the increasing broadness of the events within a plane. Fig. 10a displays the average values for the momentum p and its parallel ($p_{||}$) and transverse (p_T) component with respect to the jet axis. As can be seen $p_{||}$ increases

[2] In the region $0 < y < 0.1$ the systematic errors are substantial, so this region is not considered in this ratio

[3] Both the String-model without hard gluon emission and the Independent Jet Model with and without QCD-corrections fail to describe this effect.

[1] To match the conventions used in e^+e^--annihilations the sum of both hemispheres was used for the pp-case

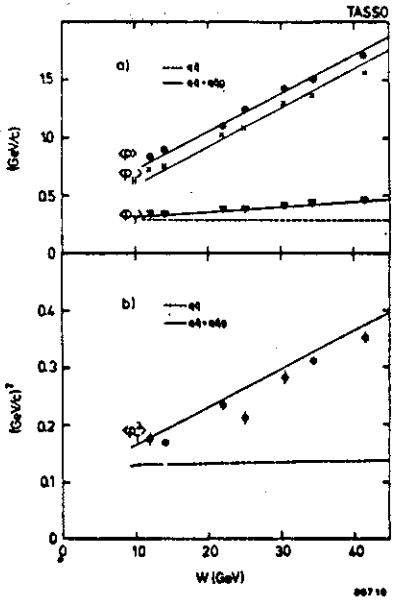

Fig.10

by roughly a factor 2.5 going from W=14 GeV to W=41 GeV, while the transverse momentum increases only weakly ($\sim$ 30%). These two features indicate that particles are collimated in jets. However simple two-jet production would not lead to the increase in $< p_T >$ as is seen from the model calculations shown in fig. 10. Such an increase can be naturally explained by hard gluon emission. This interpretation is underlined by the behaviour of the second moment of p_T : $< p_T^2 >$ increases much stronger than $< p_T >$ indicating that the rising transverse momentum is due to high momentum particles.

Motivated by findings in $pp/p\bar{p}$ -collisions (e.g. [16]) that the $< p_T >$ in minimum bias events increases with the multiplicity, the TASSO-collaboration made a similar study for different c.m. energies W. The preliminary results are shown in fig. 11. The $< p_T >$ rises with W for all multiplicities as expected from the QCD-correction, however the dependence of $< p_T >$ on the multiplicity is more complicated : it decreases with n_{CH} for W smaller and increases for W larger than than $\sim 30 GeV$.

To understand this pattern we consider the various contributions to the p_T-spectrum :

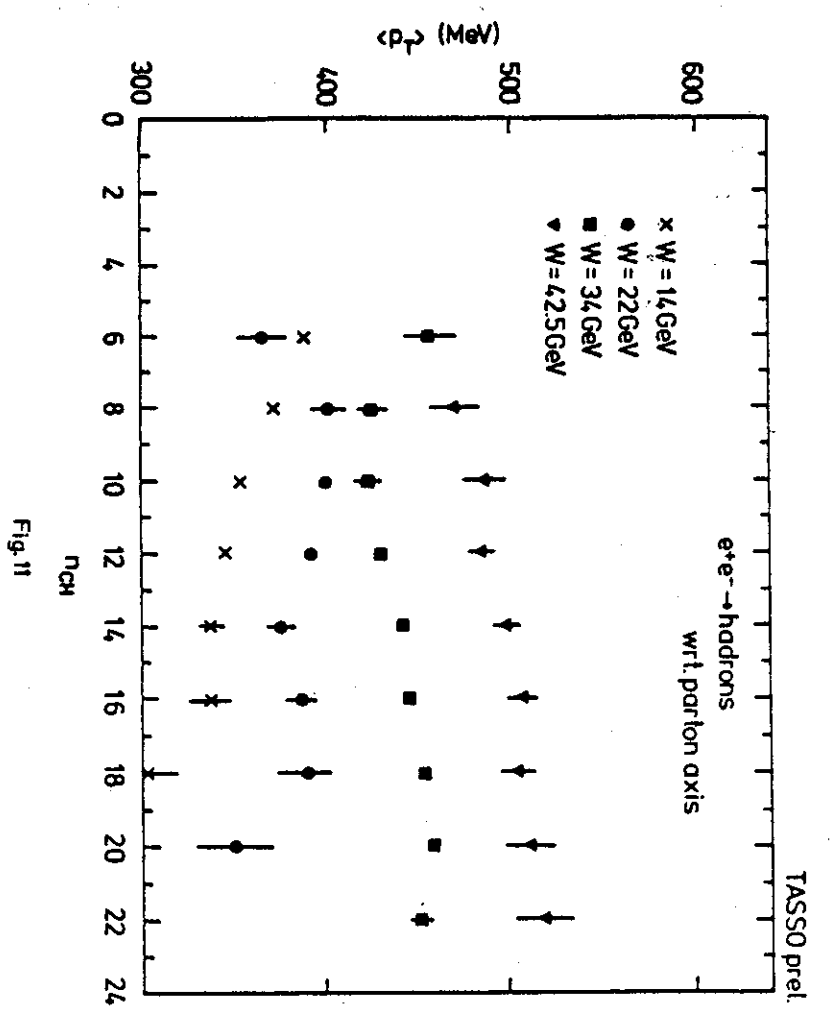

Fig.11

a. In the fragmentation process the particles get some 'intrinsic' p_T which is of the order 360 MeV (fig. 12 a). This p_T is assumed to be independent of the rank inside the fragmentation chain[1] and of the energy.

b. Decays tend to decrease the p_T of the measured particles. In the rest system of the decaying particle the decay products have a p_T of typically $\sim 250 MeV$, less than the intrinsic p_T.

c. Hard gluon emission leads to particles with a high p_T (see discussion above) exceeding the intrinsic p_T.

These three effects are generally believed to determine the p_T-spectrum of

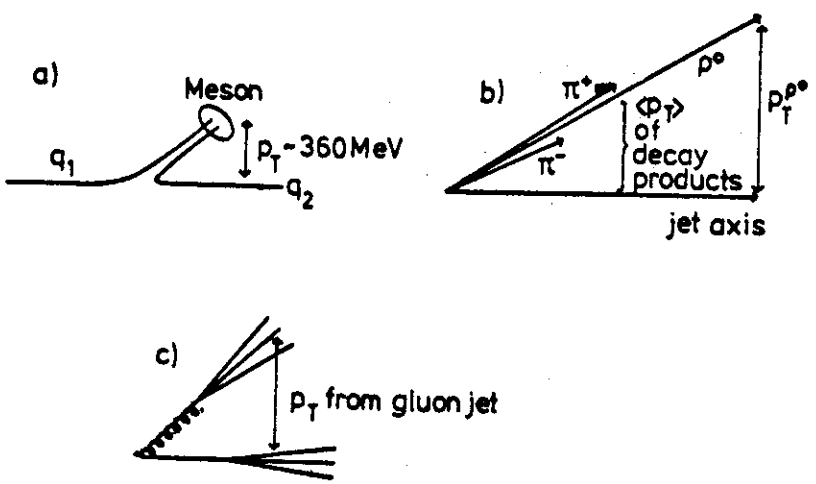

Fig.12

particles. Their relative importance depends on the multiplicity and the c.m. energy. Schematically a small multiplicity is correlated with a small fraction of particles coming from decays or hard gluon emission, a high multiplicity is expected for a high rate of decays and/or QCD-effects. At low energies hard gluon emission is not important, at W > 30 GeV it is quite abundant. Combining these

[1]Some experimental support for this assumption comes from the analysis of charmed events and will be discussed in the last section of this report

arguments one is lead to a qualitative picture consistent with the measurement.[1] For low multiplicity and low W, $< p_T >$ is goverened by the intrinsic p_T, for high multiplicity and low W, $< p_T >$ is reduced due to the large fraction of decays. For high W the gluon-bremsstrahlung becomes important, its fraction in the events increasing with multiplicity, so the $< p_T >$ should be generally larger than for W = 14 GeV and increasing with n_{CH}. The analysis shows that the p_T-spectrum involves both kinematical and dynamical effects, and it is therefore important for an interpretation of the measurements to consider both of them.

Where fragmentation ends - Bose-Einstein correlations.

Once the quarks have turned into mesons these have to obey bosonic symmetrisation properties. This leads to the Bose-Einstein effect [17], which thus allows limits to be set on the space-time region of fragmentation and allows the pion source to be explored. The experimental results will be shown after a brief discussion of the Bose-Einstein effect.

Assume two pointlike pion sources A,B. In case of equal chargesand incoherent

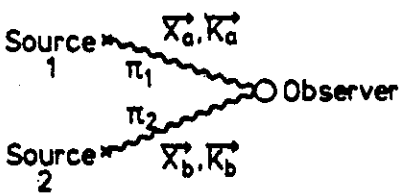

production the total wavefunction at the observer must be symmetric under the exchange of the two momenta

$$\psi = \frac{1}{\sqrt{2}}\{\psi(k_a, k_b) + \psi(k_b, k_a)\}$$

which leads to the ratio in the production of like charged to unlike charged pions

$$R^{point} = \frac{N^{++,--}}{N^{+-,-+}} \propto 1 + cos(\Delta\vec{k}\Delta\vec{x})$$

with

$$\Delta\vec{k} = \vec{k}_a - \vec{k}_b, \Delta\vec{x} = \vec{x}_a - \vec{x}_b,$$

and $N^{++,--}$ is the number of equal charged combinations, $N^{+-,-+}$ the number of unequal charged pion pairs. The functional form depends on the shape of the pion source, e.g. a gaussian distribution of this source leads to

$$R^{gauss} = \frac{N^{++,--}}{N^{+-,-+}} \propto 1 + exp\{-(\Delta\vec{k}\Delta\vec{x})^2\}$$

[1]This argumentation is supported by model calculations

and the magnitude of the effect depends on the coherence [18] between the pion-emission

$$R = 1 + \alpha exp\{-(\Delta\vec{k}\, r_0)^2\}$$

where α is maximal for a completely chaotic source (n being the number of particles considered per combination) and $\alpha = 0$ for complete coherence, $r_0 = \Delta\vec{x}$ being the radius of the source.

The preliminary data to be presented here have been obtained with the TASSO-detector [19] for 34 GeV $< W <$ 38 GeV. In the analysis all particles are treated as pions and no discrimination between prompt pions and pions from decays was attempted.

Fig. 13 displays the measured R, the ratio of like charged to unlike charged particles, for two-particle combinations (a) and three-particle combinations (b). The distance between the particles is parametrised by the Lorentz-invariant quantity

$$Q^2 = M^2 - n^2 m_\pi^2$$

where M is the invariant mass of a n-particle combination and m_π the pion-mass. For n = 2 the data show a slight increase with Q^2 above $1 GeV^2$, the dip around $Q^2 \sim 0.5\ GeV^2$ is due to the ρ^0-resonance. Going lower in Q^2 R suddenly increases for $Q^2 < 0.1 GeV^2$, giving evidence for the Bose-Einstein effect. Also shown is the result of a fit

$$R \propto (1+\gamma Q^2)(1 + \alpha e^{-\beta Q^2})$$

which describes the data quite well; the values for α and β are listed in table 1.

Fig. 13b shows the data for n=3 particle combinations together with the fit result. The increase at low Q^2 is clearly visible.

n pions	α	$\beta(Gev^{-2})$	$r_0(fm)$
2	0.30±0.04	19.5±4.	0.86±0.10
3	0.80±0.09	5.2±0.7	0.45±0.02

Table 1. Fit results for Bose-Einstein effect

As will be discussed later, quantum numbers are compensated in a small region in momentum space within e^+e^--jets. This leads to a decrease of R for

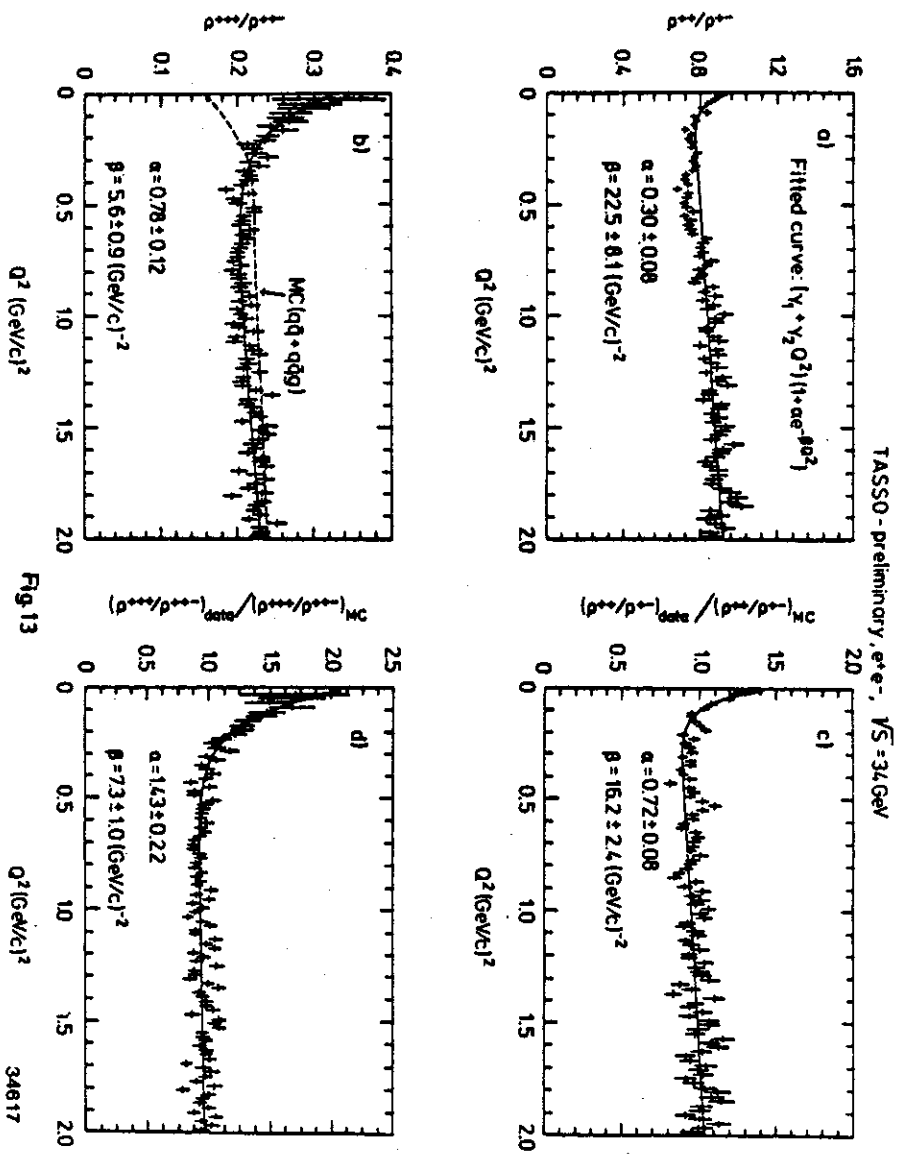

Fig. 13

$\Delta\vec{k} \to 0$. This feature was partly taken into account by normalising the measured R to the R expected from Monte-Carlo calculations[1] .

The corresponding results are shown in fig. 13 c and d. The increase at low Q^2 becomes more prominent.

Table 2 lists the result of the fit for the case n=2 and n=3.

n pions	α	$\beta(Gev^{-2})$	r_0 (fm)
2	0.46±0.04 ± 0.10	18.3±2. ± 6.	0.84±0.06 ± 0.15
3	1.18±0.18 ± 0.20	7.1±0.8 ± 3.	0.52±0.03 ± 0.12

Table 2. Fit results for Bose-Einstein effect. Data normalised to Monte-Carlo prediction

The results coincide with the values in table 1. Within the statistical and systematical errors the radii for the two cases are in agreement and limit the space-time region of fragmentation to 0.5 - 1 fm. The coherence parameter α is less than the maximum allowed value, indicating substantial coherence. Note however that as no pion identification was attempted, the measured R-value is only a lower bound due to e.g. $\pi^+ - K^+$-combinations included in the data; this should not account for more than $\sim 10\%$.

It is interesting to compare the strength and radius of the Bose-Einstein effect for different data-samples. For example the coherence may be different for two-jet events and three-jet events, or the emission radius may depend on the multiplicity as was found for ISR-data [20]. However, as can be seen from table 3 the selection of special types of events lead to consistent results - no dependence on the event sphericity[1] ($S < .1$ enriches the two-jet fraction) or the multiplicity was found. Some difference seems to occur in the coherence of particles emitted along or perpendicular to the jet axis: particles emitted transverse are more coherently produced. However the statistical significance is marginal.

[1]None of the standard fragmentation models includes the Bose-Einstein effect

[1]The sphericity S measures the jettiness of an event, $\vec{s}$ represents the jetaxis

$$S = \min_{\vec{s}}\left(\frac{\sum p_T^2}{\sum p^2}\right)$$

$S = 0$ corresponds to extreme two-jets, $S = 1$ to isotropic events.

selection	α	$\beta(Gev^{-2})$	$r_0(fm)$
all events,all pions	0.55±0.04	14.8±1.7	0.76±0.04
S≤ 0.1	0.54±0.06	14.4±2.4	0.75±0.05
$n_{CH} \geq 15$	0.52±0.06	15.0±2.6	0.77±0.05
$\Delta E_\pi < 0.3GeV$	0.58±0.10	15.6±4.0	0.78±0.08
S≤ 0.1, $\lvert cos(\Delta\vec{k}, \vec{S})\rvert \geq 0.7$	0.25±0.10	16.8±7.7	0.85±0.39
S≤ 0.1, $\lvert cos(\Delta\vec{k}, \vec{S})\rvert \leq 0.3$	0.59±0.10	12.7±3.0	0.64±0.15

Table 3. Fit results for Bose-Einstein effect applying cuts on events and particles

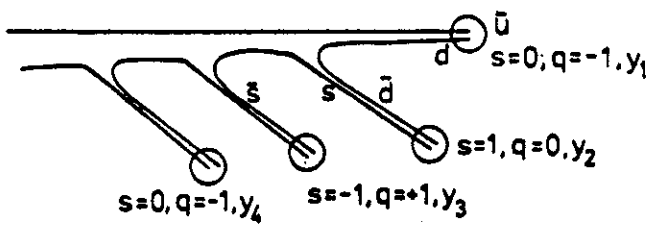

Fig. 14

A look inside jet development.

The Bose-Einstein effect is due to the interference of mesons, i.e. happens in a space-time region where the quarks have already turned into hadrons. Information on the development of a jet can be obtained e.g. by isolating particles produced at a certain rank. The first measurement of this kind will be discussed at the end of this section. Another method is to study how quantum-numbers are compensated inside a jet. E.g. the Feynman-Field idea [21] of fragmentation is sketched in fig. 14. In this picture the produced meson picks up a certain fraction of the energy that is left over and statistically

$$y_1 > y_2 > y_3 > .....$$

This leads to the expectation that quantum numbers are conserved locally, i.e. a meson with strangeness +1 is found in the vicinity of a meson with strangeness -1. In addition to this short range effect the leading particles of the two-jets (at high $|y|$) are expected to contain the primary produced quark and thus are expected to have opposite quantum numbers.

For the electric charge this leads to events which are schematically shown in fig. 15a-c, where it is assumed that two particles with opposite charge are produced per rapidity intervals and only the leading particles are singly produced at high $|y|$. To analyse the charge correlation one defines a 'test charge' at y', sums over all possible combinations with the other charged particles at any interval y and defines the charge-combination asymmetry

$$A(y',y) = \frac{N^{+-,-+}(y',y) - N^{++,--}(y',y)}{N^{+-,-+}(y',y) + N^{++,--}(y',y)} \quad .$$

In the case of the schematic event this leads to an A(y',y)- distribution as shown in figs. 15 d and e: defining the test interval in the centre of an event, the short-range charge compensation induces a peak at $y \approx y'$. Putting the test interval at the position of the leading particle in one hemisphere, a peak at $y \approx -y'$ appears due to the emission of primary quarks.

Fig. 16 shows a measurement [19][1] , where the test intervals were taken to be

$$0 \geq y' \geq -0.75, \quad -0.75 \geq y' \geq -1.5, \quad -1.5 \geq y' \geq -2.5, \quad -2.5 \geq y' \geq -5.5$$

The data show qualitatively the same behaviour as the example. A broad maximum is found for all test intervals in the region $y \sim y'$ giving evidence for short range compensation. However it is not obvious how to interpret this effect. It can be caused either by abundant resonance decays or by the inherent fragmentation mechanism. Both will lead to about the same width for the signal and it is experimentally very difficult to discriminate between these two cases from charge correlations. As will be discussed soon, other quantum numbers give a better handle on that problem.

In addition to this short range effect the anticipated long range charge compensation can also be seen. As the test interval y' is shifted towards high negative rapidities A becomes more positive for increasing y,. i.e. more oppositely charged particles are seen at a large distance from the test charge. This supplies further evidence for the production of primary produced oppositely charged partons.

As was discussed above, the positive charge correlation in the vicinity of the trigger particle can either be due to decay products or due to the inherent mechanism of fragmentation itself. A better way to discriminate between these two effects is offered by the compensation of baryon number. Resonance decays (into a baryon-antibaryon pair) are unimportant in this case. In fig. 17 the correlations between $p\bar{p}$ pairs measured by the TASSO-collaboration [23] are compared with model calculations. Used as variables are (a) the cosine of the angle θ in space

[1]Similar results have been obtained by the PLUTO [22] -collaboration

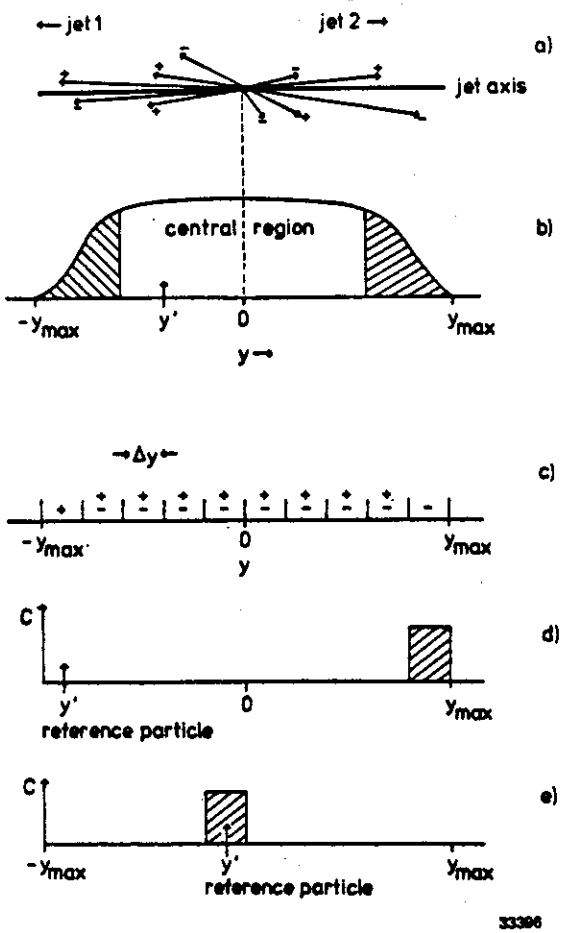

Fig.15

between the p and the $\bar{p}$, (b) the angle ϕ between $\mathring{p}$ and $\bar{p}$ in the plane orthogonal to the jet direction and (c) the difference in rapidity values : $\Delta y = |y_p - y_{\bar{p}}|$. The models belong to two classes. The model by Černy et al. [24] (dashed-dotted curve) realises a statistical concept on the quark level : quarks and antiquarks are randomly distributed in rapidity and a baryon is formed if three quarks are closest to each other. The other two models by T.Meyer [25] (full curve) and the

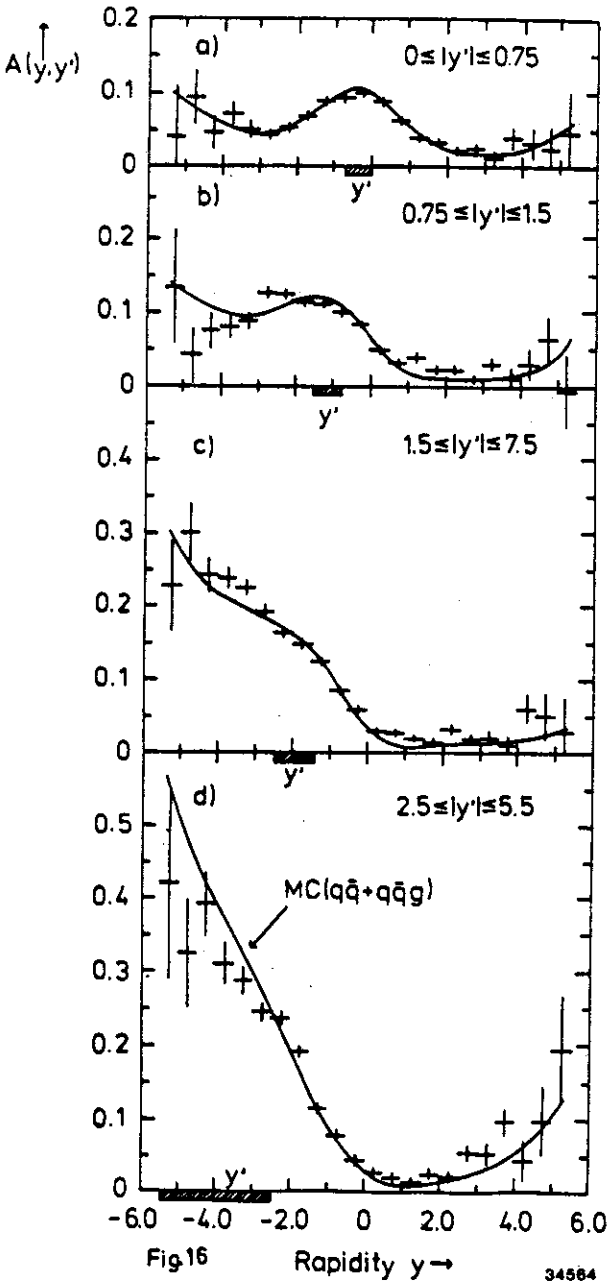
A(y,y')
a)
0≤|y'|≤0.75
b)
0.75≤|y'|≤1.5
c)
1.5≤|y'|≤7.5
d)
2.5≤|y'|≤5.5
MC(qq̄+qq̄g)
y'
Rapidity y→
34564

Fig.16

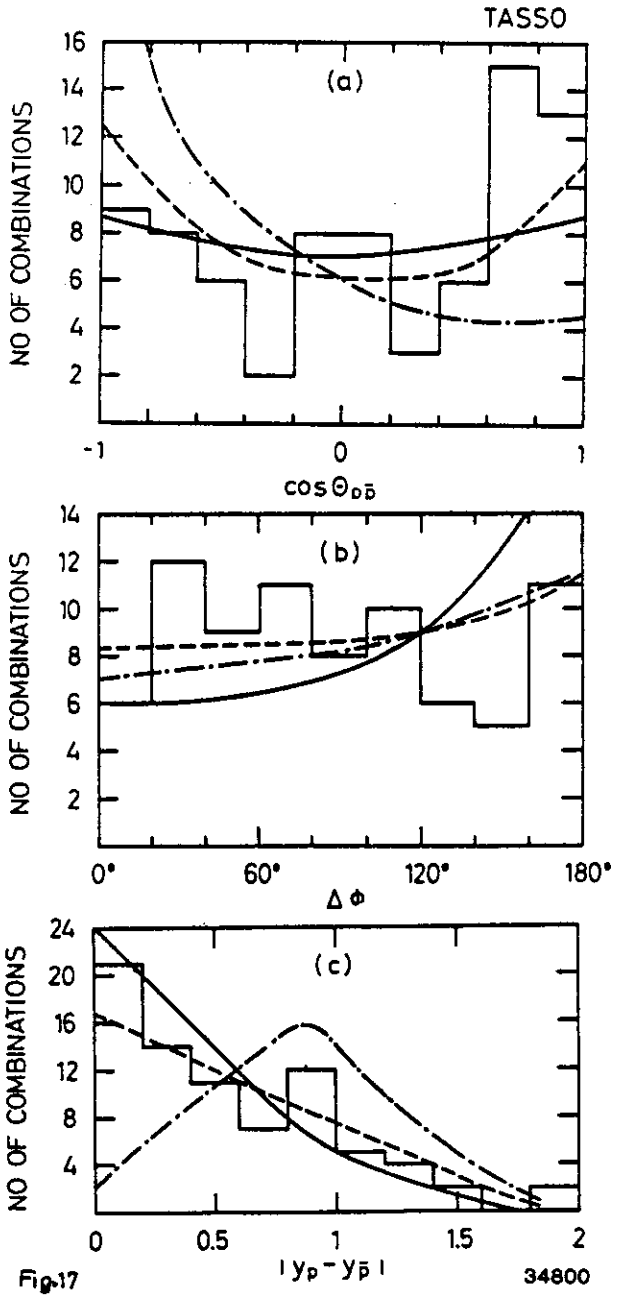
TASSO
(a)
NO OF COMBINATIONS
cos Θpp̄
(b)
NO OF COMBINATIONS
Δ Φ
(c)
NO OF COMBINATIONS
|yp − yp̄|
34800

Fig.17

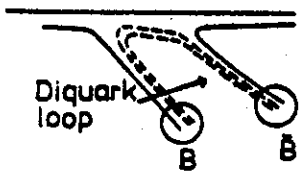

LUND-group (dashed curve) are based on the Feynman-Field type fragmentation where instead of a pair of quarks a pair of diquarks is produced. These models lead to a short range baryon number compensation. The prediction of the 'diquark' models agrees quite well with the measurement; however the statistical model fails to reproduces the trend of the data. This supports the existence of a short range compensation in jet fragmentation. This result is confirmed by additional measurements on $p\bar{p}$-pairs extending over a larger rapidity interval [**26**], on $\Lambda\bar{\Lambda}$ -pairs from several experiments [**27**,28,29] and on $\Lambda\bar{p}$-pairs [**27**]. Each of these experimental results on its own may only have a marginal significance; however, putting them all together establishes short- range quantum number compensation on firmer ground.

Note that the measurement of $\Delta\phi$ should be sensitive to local transverse momentum compensation : if the transverse momentum of a hadron is balanced by the subsequently produced particle, an accumulation of $p\bar{p}$-pairs at $\Delta\phi \sim 180$ degrees is to be expected. Such a behaviour is not seen in the data

The detection of charmed particles (D^*) in e^+e^--jets has revealed new insights on the fundamental properties of quarks [**30**]. E.g. it allowed the weak couplings of charmed quarks to be measured. In addition it offers the possibility of analysing special features of fragmentation. Charmed quarks can only be produced in the first step of jet production, coupling directly to the photon (contributions from the $b \rightarrow c$-decay can be suppressed with cuts on $x = E_{D^*}/E_{beam}$).

This can be exploited to determine the p_T-distribution of those particles which have not decayed with respect to the parton axis. The measured distribution can be well parametrised by

$$\frac{d\sigma}{dp_T^2} \propto exp{-p_T^2/2\sigma_{D^*}^2}$$

giving $\sigma_{D^*} = 0.36 \pm 0.02 GeV/c$ [**31**]. This result can be compared to $\sigma_\Lambda = 0.38 \pm 0.04 GeV/c$ [**27**] for Λ-production and a fit to the measured distribution summing over all charged particles and using a Monte-Carlo calculation to include effects from fragmentation and decays yielding $\sigma_{all} = 0.36 \pm 0.01 GeV/c$ [**32**]. Thus there is no dependence of the p_T-distribution on the mass of the considered particle and the rank in the fragmentation chain.

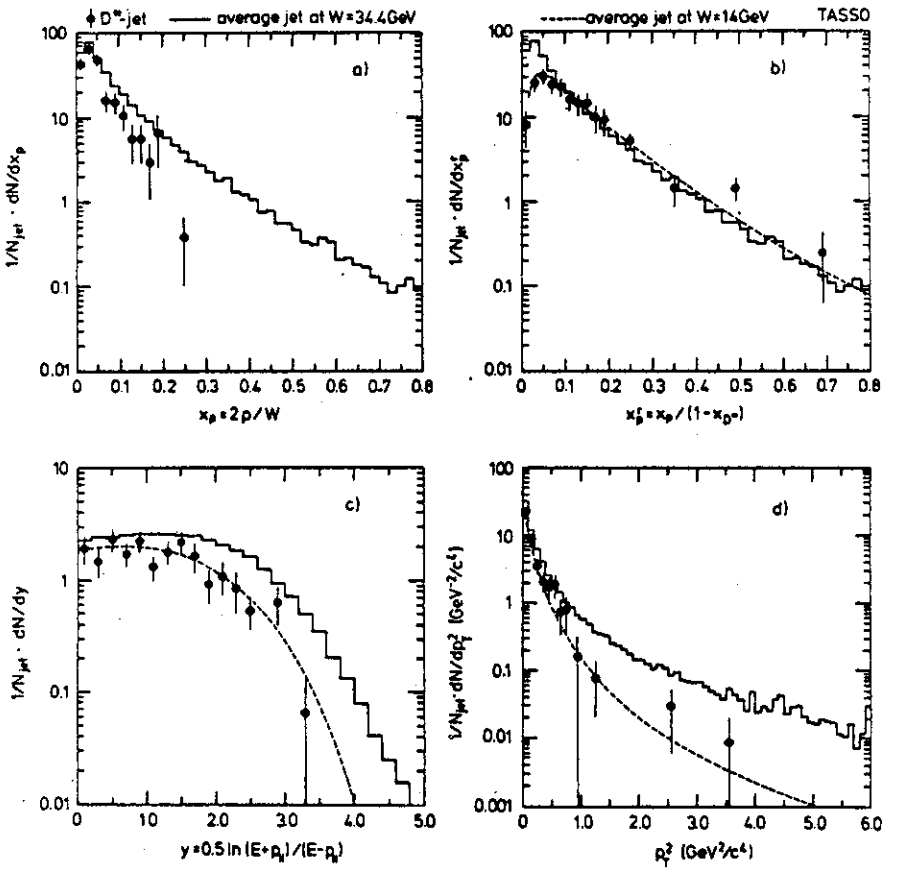

Fig.18

The separation of the meson which contains the first produced quark allows to test one of the basic assumptions of the Feynman-Field -like fragmentation: quarks fragment with a scale set by the energy left over from the earlier fragmentation steps.

For the analysis [30] the events with a tagged D^* were seperated into two hemispheres, the D^*-hemisphere and the unbiased charmed hemisphere, with

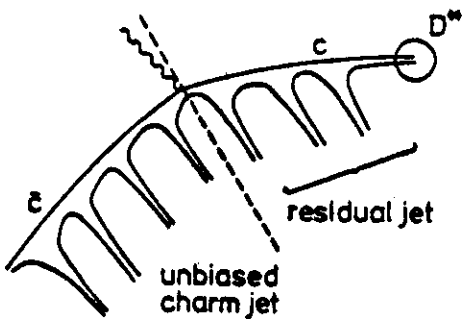

respect to the jet axis [31]. All particles in the D^* hemisphere with the exception of the D^* itself were considered as the 'residual jet'. The energy of this residual jet is

$$E_{RES} = W/2 - E_{D^*}.$$

In the data-sample considered its average value is $< E_{RES} >= 6.2\ GeV$. To test the cascade-like mechanism the distributions of the residual jet were compared with the measured distributions of a jet produced at $E_{jet} = 17GeV$ and $E_{jet} = 7GeV$, an energy close to that of the average residual jet. The results are shown in fig 18. For all distributions $x = \frac{E_{had}}{E_{jet}}$, $x_r = \frac{E_{had}}{E_{RES}}$, rapidity y and p_T^2 with respect to the jet axis, the residual jet disagrees with the jet produced at 17 GeV. Partly this may be explainable by phase space, however phase space should e.g. not influence the particle yield at low rapidities, but also here the residual jet differs from the 17 GeV-jet. In contrast to this, the comparison with a jet at 7 GeV gives a striking agreement with the residual jet and thus strongly supports the idea of a cascade like fragmentation.

Summary.

Measurements in e^+e^--annihilation by now give precise and easily interpretable information on jets and offer the basis for an understanding of fragmentation in general. Although no consistent theoretical description has been found for

fragmentation, its basic features are in remarkable agreement with simple ideas derived from the quark model and QCD.

It is obvious that the minimum bias jets in pp-collisions are different from e^+e^--jets at the same nominal W. This can be seen from the comparison of multiplicities in both reactions. Scaling violation in the KNO-distribution within the region of the rapidity plateau has been found in pp-collissions as well as in e^+e^--annihilation, the $< p_T >$ in both reactions depends on the multiplicity. In the case of e^+e^--annihilation both features can be well described by the standard fragmentation models if QCD-bremsstrahlung is included.

Bose-Einstein correlations are also found in e^+e^--annihilations showing that particles are emitted with substantial coherence and that the fragmentation occurs within 0.5-1 fm.

The new aspect of the recent analyses is the possibility to look into the development of a jet in more detail. Enough experimental data are now available to study the compensation of quantum numbers and D^*-tagging allows a direct look into the space-time development of a jet. The measurements exclude a purely statistical distribution inside the jet but show short range quantum-number compensation and support the idea of a cascade-like fragmentation.

Acknowledgement.

I am grateful for enlightening discussions with many people, particularly with W. Koch and G. Wolf. M. Dittmar, A.Eskreys and B.Foster made very useful comments on the manuscript.

For the lively and inspiring atmosphere during the workshop in Bad Honnef I especially want to thank the organisers D.K.Scott and R.M.Weiner.

References

1. S.Yamada, *talk given at the XXIInd International Conference on High Energy Physics 1984, Leipzig, GDR.*

   TASSO-collaboration, M.Althoff et al., Phys. Lett. **138B** (1984), 441.

2. For the first two sections see TASSO-collaboration, M.Althoff et al., Z.Phys.C, Particles Fields **22**, 307.

3. E. Albini et al., Nuov. Cim. **32A** (1976), 101.

4. J.D.Bjorken, S.J.Brodsky, Phys. Rev. **D1** (1970), 1416.

   W. Ochs, MPI Munich preprint MPI-PAE 118 (1983).

5. A.Bassetto, M.Ciafaloni, G. Marchesini, Phys. Lett. **83B** (1978), 207.

K.Konishi, Rutherford preprint, RL 79-035 (1979).

W.Furmanski,S. Pokorski, Nucl. Phys. **115B** (1979).

A.H.Mueller, Phys. Lett. **104B** (1981), 161.

6. Z.Koba, H.B.Nielsen, P.Olesen, Nucl. Phys. **B40** (1972), 317.
7. JADE-collaboration, W.Bartel et al., DESY report 83-042 (1983).
8. J.M.Weiss (HRS-coll.), *Proc. of SLAC Summer Institute 1983, Stanford.*
9. W.Koch, *in Proc. of the XIIIth International Symposium on Multiparticle Dynamics, Voldendam, the Netherlands.*
10. W.Hofmann (PEP4-TPC coll.), *in Proc. of SLAC summer Institute 1983, Stanford.*
11. P.Hoyer et al., Nucl. Phys. **B161** (1979), 34.
12. B.Barish (DELCO-coll.), *talk given at the XXIInd International Conference on High Energy Physics 1984,.*
13. B.Andersson, G.Gustafson, T.Sjoestrand,, Phys. Lett. **94B** (1980), 211.
14. A.Bassetto et al., Nucl. Phys. **B207** (1982), 189.

Y.L.Dokshitzer, V.S.Fadin, V.A.Khoze, Phys. Lett. **115B** (1982), 242.

B.R.Webber, CERN-report TH-3713 (1983).

15. K. Böckmann, these proceedings.
16. UA1-collaboration, G. Arnison et al., Phys. Lett. **118B** (19982), 167.
17. G. Goldhaber et al., Phys. Rev. **120** (1960), 300.
18. G.N.Fowler, R.M.Weiner, Phys. Lett. **70B** (1977), 201.
19. TASSO-coll., M.Althoff, to be published.
20. AFS-coll., T.Åkesson et al., Phys. Lett. **129B** (1983), 267.
21. R.D.Field, R.P.Feynman, Nucl. Phys. **B136** (1978), 1.
22. PLUTO-coll. Chr. Berger et al., DESY-report 82-058.
23. TASSO-coll., M.Althoff et al., Z.Phys.C, Particles Fields **17**, 5.
24. V.Černy, P.Lichard, J.Pisut, Phys. Rev. **D16**, 2822; Acta Phys. Polonica **B10**, 629; Phys. Rev. **D18**, 2409; Czech.J.Phys. **B31**, 1302.
25. T.Meyer, Z.Phys.C, Particles Fields **12**, 77.
26. TASSO-Coll. M.Althoff et al., Phys. Lett. **139B**, 126.